NONLINEAR PREDICTIVE CONTROL OF AN INDUSTRIAL SLURRY REACTOR

C. H. Fontes[*]
cfontes@ufba.br

M. J. Mendes[†]
mendes@desq.feq.unicamp.br

[*]Programa de Pós-Graduação em Engenharia Industrial (PEI), Escola Politécnica,
Universidade Federal da Bahia,
Salvador, Bahia, Brazil

[†]Faculdade de Engenharia Química, Universidade Estadual de Campinas,
Campinas, São Paulo, Brazil

ABSTRACT

A nonlinear model predictive control (NMPC) is applied to a slurry polymerization stirred tank reactor for the production of high-density polyethylene. Its performance is examined to reach the required mean molecular weight and comonomer composition, together with the temperature setpoint. A complete phenomenological model including the microscale, the mesoscale and the macroscale levels was developed to represent the plant. The control algorithm comprises a neural dynamic model that uses a neural network structure with a feedforward topology. The algorithm implementation considers the optimization problem, the manipulated and controlled variables adopted and presents results for the regulatory and servo problems, including the possibility of dead time and multi-rate sampling in the controlled variables. The simulation results show the high performance of the NMPC algorithm based in a model for one-step ahead prediction only, and, at the same time, attests the strong difficulty to control polymer properties with dead time in their measurements.

KEYWORDS: Olefin Polymerization, Predictive control, neural networks.

RESUMO

Uma estratégia de controle preditivo não linear é aplicada a um reator tanque agitado de polimerização em lama para a produção de polietileno de alta densidade. O desempenho do controle é analisado no sentido de se obter o peso molecular médio numérico, composição de comonômero e temperatura desejados. Um modelo fenomenológico completo considerando as micro, meso e macro escalas de modelagem foi desenvolvido para representar a planta. O algoritmo de controle compreende um modelo interno baseado em redes neurais com topologia "feedforward". A implementação do algoritmo contempla o problema de otimização, as variáveis manipuladas e controladas adotadas e são apresentados resultados para os casos de problema servo e regulatório, incluindo-se a possibilidade de tempos mortos e múltiplas taxas de amostragem nas variáveis controladas. Os resultados de simulação mostram o bom desempenho do algoritmo NMPC baseado em um modelo neural treinado para a predição da variável de saída apenas um instante de tempo a frente e, ao mesmo tempo, atestam a dificuldade de controlar diretamente as propriedades do polímero com a ocorrência de tempo morto na medição.

PALAVRAS-CHAVE: Polimerização de olefinas, controle preditivo, redes neurais.

Artigo submetido em 29/03/2007
1a. Revisão em 16/07/2008
2a. Revisão em 04/08/2008
Aceito sob recomendação do Editor Associado
Prof. José Roberto Castilho Piqueira

1 INTRODUCTION

In the polymerization industry, there is considerable incentive to develop real-time optimal strategies that will result in the production of polymers with desired molecular properties. In this sense, the production of polymers with specified end-use properties means that process variables such as temperature and molecular weight must be controlled.

The difficult to measure controlled variables, the existence of interactions, dead time and constraints, added to the nonlinear and multivariable nature (Schork et al., 1993, Ozkan et al., 2001), pose a challenger problem for the control of polymerization reactor. In many plants, there is a heuristic strategy to control the output process variables. The development of control strategies for polymerization reactors requires an appreciation of what the important properties are and how they relate to variables within the reactor and furthermore, what inputs are available. Penlidis et al. (1992) show that simple models that do not require a heavy computational load but capture all the essential process features, are easily amenable to reactor optimization and control studies.

Model Predictive Control (MPC) refers to a class of algorithms that compute a sequence of manipulated variable adjustments in order to optimize the future behavior of a plant. In recent years, there is a considerable literature on the MPC technology, including overviews, industrial applications and its main features (Qin and Badgwell, 1997, 2000, Diehl et al., 2002).

Continuous polymerization processes, such as slurry technology, appear to be suitable for the model predictive control (Rovaglio et al., 2004, Jeong et al., 2001) because, among other things, these processes are multivariable, tightly constrained and typically present a "fat" control problem (Qin and Badgwell, 1997, Schnelle and Rollins, 1998) with more manipulated variables (MV's) than controlled variables (CV's), which suggests opportunities for process optimization also. The nonlinear nature and the large operating regimes with multi-grade productions led to the development of nonlinear model predictive control (NMPC) in which a more accurate nonlinear model is used for process prediction and optimization (Henson, 1998).

Some references present the application of the advanced control algorithms in polymerization systems. Ibrehem et al. (2008) worked with olefin polymerization (ethylene polymerization) in fluidized-bed catalytic reactors. The authors developed a complete model that takes into account mass and heat transfer between the solid particles and surrounding gas in the emulsion phase, and also present the application of neural-network based predictive control for controlling the temperature of the emulsion system. Other recent work (Gandhi and Mhaskar, 2008) considers the problem of control a styrene polymerization process subject to input constraints and destabilizing faults in the control actuators. For the batch and semi-batch polymerization reactors in particular, additional difficulties arise concerning process variables, such as reactor temperature and pressure, which have to follow set-point trajectories to assure the quality of the final product. Fontes et al. (2006) show the results and procedures associated with the application of a fuzzy control strategy in a semi-batch reactor for the production of nylon 6, including variable set-points for pressure and temperature. Nagy et al. (2007) present the benefits of nonlinear model predictive control (NMPC) for the setpoint tracking control of an industrial batch polymerization reactor, considering. According to the authors, two different control problems arise in batch process operation, namely, the end-point property control, associated to the product quality at the end of the batch, and the setpoint tracking, associated to the time-varying setpoint trajectories. Some references are related to the control of particle size distribution. Dokucu et al. (2008) developed strategies for the regulation of the particle size distribution in a semibatch vinyl acetate (VAc)/butyl acrylate emulsion polymerization system. Three integrated strategies that exploit model reduction to control the PSD (Particle Size Distribution) are presented and compared. The same polymerization system was adopted to test a multi-rate model predictive controller algorithm to control the full particle size distribution (Dokucu et al., 2008). Embiruçu and Fontes (2006) presented closed-loop results related to the same system described in Figure 1 considering, in this case, Ziegler-Natta and Phillips catalysis. The authors suggest an approach for the generalized predictive control algorithm, a linear predictive controller, to consider multiple sampling rates in the controlled variables.

This work presents the computational implementation of a predictive control algorithm with nonlinear internal model applied to an industrial copolymeritzation reactor of ethylene (monomer) and 1-buthene (comonomer) with Ziegler-Natta catalysis. Figure 1 represents schematically the reactor. The process comprises the production of high density polyethylene in stirred tank reactor. Together with ethylene and 1-buthene, hydrogen, nytrogen and n-hecane (solvent), catalyst and cocatalyst (both in n-hexane solution) are fed continuously. The polymer is insoluble in the solvent and the slurry is discharged for posterior drying. The reaction is exothermic, the system is open loop unstable, and the reactor temperature control comprises heat exchange in the reactor jacket and slurry cooling in external heat exchangers. The polymer chain growth mechanism is the coordination polymerization. The process depicted is related to the commercial plant of Braskem Petrochemical Company placed at Petrochemical Complex of Camaçari (Brazil). An identification work, using correlation analysis, was accomplished in this same industrial system (Fontes and Embiruçu, 2001).

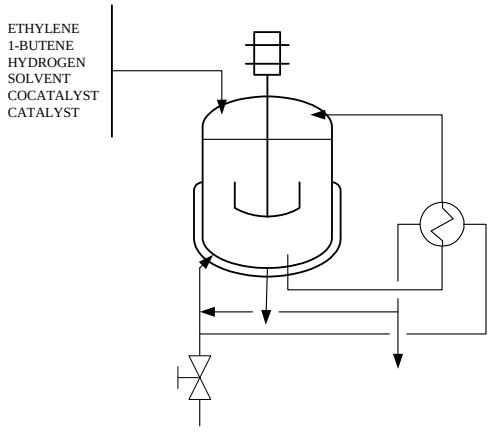

Figure 1: Schematic representation of the reactor.

The actual state of this process comprises the control of reactor temperature and the trial of control the melt index through an heuristic procedure that includes the adjustment of hydrogen/ethylene ratio in the reactor gas phase. The inexistence of a systematic treatment, the intrinsic complexity of a polymerization process, marked by its multivariable nature, do not warrant the specification of product with melt index values inside acceptable limits. In this sense, this work treats a control problem that represents an expected increase in the control technology applied to the process described. The control problem comprises the need of expressive reduction in the molecular properties variability through a multivariable strategy that considers all effects on these properties and establishes directly setpoints for these.

This work presents the problem formulation and simulation results based on a complete phenomenological model of the system (Fontes and Mendes, 2005). An analysis of degree of freedom of this model suggested the establishment of three control variables. In accordance with the process reality and the control problem presented, two polymer properties (average molecular weight and copolymer composition), outputs of phenomenological model, were consider together with the slurry temperature. Additional challenges such as dead time and multi-rate sampling must be analyzed also owing to the direct control of two polymers properties simultaneously with reactor temperature, whose time constant is much smaller than others.

The optimization problem and simulation results for the regulatory and servo (grade transitions) problems are presented. The neural model was identified to supply only one-step ahead preditions. The simulation tests comprised the analysis of additional aspects such as dead time and multi-rate sampling in the controlled varibales.

Section 2 presents the main aspects related to the phenomenological and neural dynamic models, which are treated in Fontes and Mendes (2001). Finally, section 3 presents the NMPC implementation, pointing out the manipulated and controlled variables, the optimization problem, variables scaling and simulation results.

2 METHODS

The dynamic model

Fontes and Mendes (2001, 2005) present the details about the phenomenological dynamic model used in this work. As discussed in Ray (1991), processes of the heterogeneous catalysed olefin polymerization reactors may be decomposed in three levels, namely the microscale (chemical kinetic aspects), the mesoscale (transport in the particle), and the macroscale (overall mass and energy balance equations) levels. This decomposition is used in the present work to construct the reactor model. Some simplifying assumptions were adopted such as the slurry volume constant and perfect mixing of gas and liquid phases.

At the microscale level, one kinetic mechanism was adopted, according to the coordination polymerization (Kiparissides, 1996), including initiation, propagation, chain transfer and deactivation reactions (see Table 1). Two types of catalytic sites are considered, each one with its own kinetic constants, and the concept of the terminal model for copolymerization (Soares and Hamielec, 1995, 1996) is implicit in the kinetic equations.

ET, BT and CC are ethylene, 1-butene and cocatalyst, respectively. The others symbols are commented in Nomenclature. The procedure employed at the microscale level comprised the generation of balance equations for the living $\left(P_{1_j}(n,m), P_{2_j}(n,m)\right)$ and dead polymer chains $(D_j(n,m))$, the application of the method of moments (Hutchinson et al., 1992) to enable the mathematical treatment of average polymer properties, and the obtainment of rate equations for the zero, first and second order moments. Consumption rate expressions for the ethylene, 1-butene, hydrogen, cocatalyst and active site were obtained also. The kinetic constants (Fontes and Mendes, 2001, 2005) were employed in Arrhenius equation form. Table 2 shows the values of frequency factors for the rate constants. For the activation energies of the propagation, chain transfer and deactivation steps, respectively, the values of 29.4 kJ/mol, 50.2 kJ/mol and 4.2 kJ/mol were taken.

At the mesoscale level, a non-uniform solid phase is considered and, in the particle, there is a radial distribution of chemical species such as the living and dead polymer chains. The multigrain model approach (Floyd et al., 1986) was adopted combined with a simulation strategy applying orthogonal

Table 1: Kinetic mechanism for site type j. $(j = 1, 2)$

Initiation:
$P_j(0,0) + ET \overset{K_{pee_j}}{\rightarrow} P_{1_j}(1,0)$
$P_j(0,0) + BT \overset{K_{pbb_j}}{\rightarrow} P_{2_j}(0,1)$
Propagation:
$P_{1_j}(n,m) + ET \overset{K_{pee_j}}{\rightarrow} P_{1_j}(n+1,m)$
$P_{2_j}(n,m) + ET \overset{K_{pbe_j}}{\rightarrow} P_{1_j}(n+1,m)$
$P_{1_j}(n,m) + BT \overset{K_{peb_j}}{\rightarrow} P_{2_j}(n,m+1)$
$P_{2_j}(n,m) + BT \overset{K_{pbb_j}}{\rightarrow} P_{2_j}(n,m+1)$
Chain Transfer:
$P_{1_j}(n,m) \overset{K_{ts_j}}{\rightarrow} P_j(0,0) + D_j(n,m)$
$P_{2_j}(n,m) \overset{K_{ts_j}}{\rightarrow} P_j(0,0) + D_j(n,m)$
$P_{1_j}(n,m) + H_2 \overset{K_{th_j}}{\rightarrow} P_j(0,0) + D_j(n,m)$
$P_{2_j}(n,m) + H_2 \overset{K_{th_j}}{\rightarrow} P_j(0,0) + D_j(n,m)$
$P_{1_j}(n,m) + ET \overset{K_{tme_j}}{\rightarrow} P_{1_j}(1,0) + D_j(n,m)$
$P_{2_j}(n,m) + ET \overset{K_{tmb_j}}{\rightarrow} P_{1_j}(1,0) + D_j(n,m)$
$P_{1_j}(n,m) + CC \overset{K_{tcc_j}}{\rightarrow} P_{1_j}(1,0) + D_j(n,m)$
$P_{2_j}(n,m) + CC \overset{K_{tcc_j}}{\rightarrow} P_{1_j}(1,0) + D_j(n,m)$
Deactivation:
$P_{1_j}(n,m) \overset{K_{d_j}}{\rightarrow} Cd_j + D_j(n,m)$
$P_{2_j}(n,m) \overset{K_{d_j}}{\rightarrow} Cd_j + D_j(n,m)$

collocation. One material balance on the macropartcile for each specie was developed considering that convective mass transfer inside macropartcile and the instantaneous variation of its volume are negligible.

The assumption of a non-uniform species distribution on the particle established the development of a general local balance (Fontes and Mendes, 2005), providing equations for the moments of chain length distribution and for the active site concentrations.

The macroscale comprised one mass balances for the liquid and gas phases and another for the solid phase, for each one component (ethylene, 1-buthene, hydrogen, solvent and nitrogen). Overall mass and energy balances were established also.

Table 2: Frequency factors of the kinetic constants $(1/(\text{mol.min}))$

	Site 1	Site 2
Propagation:		
$K_{p,ee}$	1.101×10^{8}	1.101×10^{8}
$K_{p,be}$	2.591×10^{6}	1.943×10^{7}
$K_{p,eb}$	8.290×10^{7}	8.290×10^{7}
$K_{p,bb}$	1.943×10^{6}	8.031×10^{6}
Chain transfer		
$K_{t,s}(\text{min}^{-1})$	1.615×10^{5}	1.615×10^{5}
$K_{t,h}$	1.421×10^{8}	1.421×10^{7}
$K_{t,me}$	3.392×10^{6}	3.392×10^{5}
$K_{t,mb}$	3.392×10^{6}	1.615×10^{5}
$K_{t,cc}$	3.876×10^{7}	3.876×10^{6}
Deactivation		
K_d	3×10^{-1}	3×10^{-1}

Despite the simulations tests, Table 3 presents the absolute initial values of all inputs variables together with initial values for the weight-average molecular weight (WAMW) and temperature.

Table 3: Initial absolute values for simulation tests.

Hydrogen feed flow	10 kg/h
Catalyst feed flow	0.075 kg/h
Comonomer feed flow	150 kg/h
Solvent feed flow	16000 kg/h
Cocatalyst feed flow	0.2 kg/h
Monomer feed flow	7500 kg/h
Water flow in the reactor jacket	150000 kg/h
Water flow in the external heat exchangers	60000 kg/h
WAMW	122000
Temperature	84.6 ^{o}C

The complete model is made of ordinary and algebraic equations. Adopting five internal collocation points in the particle, the differential algebraic system comprises 14 algebraic equations and 267 ordinary differential equations, distributed according to the Table 4. This expressive size and the long simulation time turn the phenomenological model unsuitable

for use in the predictive control applications.

Table 4: Complete dynamic model.

	Number of equations
Statistic moments Active sites balance	216 12
Macroparticle mass balances	25
Component mass balance Overall energy and mass balances	12 2
Algebraic equations	14
Total	281

The procedure adopted to obtain the neural models, used in the predictive control algorithm, is presented in Fontes and Mendes (2001). The neural network structure consists of a feedforward topology with only one hidden layer and gives one-step ahead prediction. The tangent hyperbolic function was used in the hidden neurons and the linear function was used in the output layer. The training was accomplished using the Levenberg-Marquadt algorithm with a learning rate equal to 0.01 and the initial value for the Hessian adjustment parameter was assumed equal to 0.9. A batch training procedure was applied considering the minimization of the mean squared error of each epoch.

The identification was conducted adopting one neural model for each process output that can be represented by a NARX (Nonlinear AutoRegressive with eXogeneous inputs) structure (Su and McAvoy, 1997, Doherty et al., 1997). The MISO (Multiple Input Single Output) model, for each output, considers all process inputs (feed rates of ethylene, catalyst, cocatalyst, 1-butene, hydrogen, solvent and refrigeration water), and one value of dead time for each input variable had to be adopted also. Two data samples (training and test), provided from the phenomenological model (sampling period of 5 min), were adopted for the identification and a cross validation procedure was adopted in order to select the best number of hidden neurons for each MISO model, considering a maximum number of 2000 training epochs. As it was to be expected, in the nonlinear case a neural model with a feedforward structure leads to results that are more accurate for short prediction horizons than for long prediction horizons. Multi-step ahead prediction is however necessary to implement predictive control schemes.

2.1 Nonlinear model based control algorithm

The predictive control algorithm for the slurry reactor has the following features:

- Multiple inputs and multiple controlled variables.
- Simultaneous resolution of the optimization problem.
- Internal model comprising one neural model for each control variable (MISO model) that includes all the manipulated variables adopted.

An analysis of the phenomenological model conducted to achievement of 3 degrees of freedom for this and 3 variables were selected to be controlled:

- Reactor temperature (T_r).
- Weight-average molecular weight (M_w).
- Average fraction of comonomer incorporated into the polymer (X_{BT}).

This set of controlled variables poses additional challenges for the control problem. First, there is the possibility of considerable dead time in the measurement of outputs associated with the polymer properties (M_w and X_{BT}) owing to the slurry transport, drying and the analysis time. Second, process variables such as temperature have a dynamic response typically speed regard to the polymer properties, which suggests the existence of multi-rate sampling in the controlled variables. The closed loop simulation comprised the additional analysis of these two effects (dead time and multi-rate sampling) on the control algorithm performance.

8 (eight) manipulated variables were adopted comprising feed rates to the reactor and water flows related to the refrigeration system:

- Ethylene massic flow (F_{ET}).
- Buthene massic flow (F_{BT}).
- Catalyst massic flow (F_C).
- Cocatalyst massic flow (F_{CC}).
- Hydrogen massic flow (F_{H_2}).
- N-hexane massic flow (F_{NX}).
- Water flow to the reactor jacket (F_{WC}).
- Water flow to the external heat exchangers (F_{WT}).

2.2 Optimization problem

Besides the nonlinear nature of plant, a nonlinear internal model suggests also the possibility of a more efficient controller, able to accomplish grade transitions, without changes the catalytic system. These grade transitions are common in the system studied and imply in an expressive change of the operation point.

Adopting the controlled and manipulated variables listed in the previous section, the predictive control algorithm comprises the following nonlinear programming problem, which must be solved at each sampling period to generate the control moves.

Objective function

$$\min_{u(t)} E(t) = \left(\sum_{k=1}^{P} \|e(t+k)\|_R^2 \right) + \left(\sum_{k=1}^{M} \|\Delta u(t+k-1)\|_Q^2 \right), \quad (1)$$

where the norm terms mean $\|x\|_Z^2 = x^T \cdot Z \cdot x$, and t is the current instant.

The control moves of each one MV $(u \equiv F_{ET}, F_{BT}, F_C, F_{CC}, F_{NX}, F_{H_2}, F_{WC}, F_{WT})$ are achieved as follows:

$$\Delta u(l) = u(l) - u(l-1), \text{ if } l > t, \quad (2)$$

$$\Delta u(l) = u(l) - u(t-1), \text{ se } l = t, \quad (3)$$

and the deviations from a desired response, over a prediction horizon of length P must be achieved for each controlled variable $(y \equiv T_r, M_w, X_{BT})$:

$$e(t+k) = y_{ref}(t+k) - [\hat{y}(t+k) + d], \quad (4)$$

where $d = y(t) - \hat{y}(t)$.

Despite the options for specifying future CV behavior (Qin and Badgwell, 1997), reference trajectory was adopted in this work and a first order curve is drawn from the current CV value to the setpoint according to the following expression:

$$y_{ref}(t+k) = \alpha^k \cdot y(t) + y_{sp}(t) \cdot \left(1 - \alpha^k\right), k = 1, \ldots, P \quad (5)$$

α is the time constant that establishes the response speed.

Constraints

Regarding to the input variables, the following constraints must be considered:

$$u_i \leq u(t+k-1) \leq u_s, k = 1, \ldots, M, \quad (6)$$

$$\Delta u_i \leq \Delta u(t+k-1) \leq \Delta u_s, k = 1, \ldots, M. \quad (7)$$

Hard constraints are also considered for the output predictions:

$$y_i \leq \hat{y}(t+k) \leq y_s, k = 1, \ldots, P, \quad (8)$$

where $(u \equiv F_{ET}, F_{BT}, F_C, F_{CC}, F_{NX}, F_{H_2}, F_{WC}, F_{WT})$ and$(y \equiv T_r, M_w, X_{BT})$.

The model constraints comprises the MISO neural model identified for each CV, whose structure presents all the MV's. Each CV contributes with P equality constraints expressed as follows:

$$\hat{y}(t+1) = F_y \left\{ \begin{array}{l} y(t), y(t-1), \ldots, \\ y(t-n_y+1), F_{ET}(t), \ldots, \\ F_{ET}(t-1-n_{ET_y}+2), \ldots, \\ F_{WT}(t), \ldots, F_{WT}(t-1-n_{WT_y}+2) \end{array} \right\} \quad (9)$$

$$\hat{y}(t+2) = F_y \left\{ \begin{array}{l} \hat{y}(t+1), y(t), \ldots, y(t-n_{M_w}+2), \\ F_{ET}(t+1), \ldots, \\ F_{ET}(t-1-n_{ETy}+3), \\ \ldots, F_{WT}(t+1), \ldots, \\ F_{WT}(t-1-n_{WTy}+3) \end{array} \right\} \quad (10)$$

$$\vdots \qquad \vdots \qquad \vdots$$

$$\hat{y}(t+P) = F_y \left\{ \begin{array}{l} \hat{y}(t+P-1), \hat{y}(t+P-2), \ldots, \\ y(t), \ldots, y(t-n_{M_w}+P), \\ F_{ET}(t+P-1), \ldots, \\ F_{ET}(t-n_{ETy}+P), \ldots, \\ F_{WT}(t+P-1), \ldots, \\ F_{WT}(t-n_{WTy}+P) \end{array} \right\} \quad (11)$$

The optimization problem presented has 8×M+3×P decision variables (output predictions were also considered decision variables in the problem formulation) and 8×M degrees of freedom that is equal to the number of present and future values of MV's.

2.3 Scaling variables

In the system studied, there are enormously differences in the typical values of MV's and CV's that should be considered in the penalty adjustments (weight matrices Q and R) for the control tuning (Meadows and Rawlings, 1997). In this sense, the scaling by variable transformation (Gill et al., 1981) should be useful and provides certain desirable properties during the optimization process.

All the decision variables presented in the optimization problem were scaled trough the use of dimensionless deviation variable (ddv):

$$v^{ad} = \frac{v - v_{ss}}{v_{ss}}, \tag{12}$$

where v_{ss} is the initial steady state considered in the simulation tests.

2.4 Tuning procedure

The strategy employed for the tuning parameters adjustments comprised the following aspects:

- Only the move suppression factors and horizons were adjusted.
- The penalties on the deviations from the desired response (matrix R) were fixed at 20 for all CV's.
- The time constant of the reference trajectory was fixed at 0.5 for all CV's.
- The weights of each control move and output prediction deviations were assumed constant along the prediction horizon.

The limits used for all MV's are in agreement with the data range adopted during the neural models training (section 3). Based on the melt index and density specifications and on the operational practice, bounds were established for each CV (table 5), regarding to its current setpoint.

The grade transitions simulations (servo problems) establish changes in the output bounds or specifications. In this sense, it was proposed the use of two trajectories to represent the bounds of each output during the grade transition. Considering the use of hard constraints for the CV's predictions (Eq. 8), the trajectory parameters in each case were always adjusted to reduce the effect of the output bounds on the optimization problem. Hence, in the case of setpoint increase, the upper and lower trajectories must be speedy and sluggish, respectively. In the case of setpoint decrease the opposed is applied.

Table 5: Output specifications.

Variable	Bounds
T_r	± 1 %
M_w	± 3 %
X_{BT}	± 5 %

2.5 Measurement delay in the outputs

The occurrence of a dead time equals to θ_u sampling intervals in some CV measurement leads to increase the prediction horizon owing to the inclusion of present and future MV's values only after the first θ_u output predictions. To prove this fact, consider a SISO case where the internal model is represented as follows:

$$\hat{y}(t+1) = F(u(t), y(t)).$$

Considering that y_m is the measured value from the plant and that this measurement has a delay equals to θ_u, the predictions obtained at time t are:

$$\hat{y}(t+1) = F(u(t-\theta_u), y_m(t)), \tag{13}$$
$$\hat{y}(t+2) = F(u(t-\theta_u+1), \hat{y}(t+1)) \tag{14}$$
$$\vdots$$
$$\hat{y}(t+\theta_u) = F(u(t-\theta_u+\theta_u-1), \hat{y}(t+\theta_u-1)) \tag{15}$$
$$\hat{y}(t+\theta_u+1) = F(u(t), \hat{y}(t+\theta_u)), \tag{16}$$
$$\hat{y}(t+\theta_u+2) = F(u(t+1), \hat{y}(t+\theta_u+1)), \tag{17}$$
$$\vdots$$
$$\hat{y}(t+\theta_u+P) = F(u(t+\theta_u+P-1), \hat{y}(t+\theta_u+P-1)) \tag{18}$$

In the presence of a dead time θ_u in the polymer properties measurements (M_w and X_{BT}), the strategy adopted comprised the establishment of a prediction horizon equals to P+θ_u, followed of elimination of the first θ_u predictions.

In some tests with a long prediction horizon, only a subset of predictions, called coincident points (Qin and Badgwell, 1997), is selected and used in the optimization problem.

2.6 Simulations tests and discussion

The simulation tests were conducted in two steps comprising the servo and regulatory problems. First, the controller performance was analyzed considering one grade transition without change in the catalytic system. For the regulatory problem tests, the ability to reject some potential disturbances and to keep controlled variables in their setpoints were verified.

In all tests, the process is represented by the phenomenological model (Fontes and Mendes, 2001) and the control action interval is always equals to 5 min.

2.6.1 Servo problem

In this section, simultaneous setpoint changes in the controlled variables were applied according to table 6. Changes in the specification limits were also imposed and the strategy described in section 3.3 had to be used.

Table 6: Setpoint changes (grade transition).

Variable	initial setpoint (ddv))	end setpoint (ddv)
T_r	0	0.069
M_w	0	-0.123
X_{BT}	0	0.069

The tests comprised two cases:

- Setpoint changes considering multi-rate sampling in the controlled variables. Measurement intervals of 5 min and 40 min were adopted for the temperature and polymer properties (M_w and X_{BT}), respectively.
- Setpoint changes with a dead time equals to 30 min owing to delay in the molecular weight and comonomer content measurements.

Despite the tuning procedure, an initial standard tuning was employed as a reference for the adjustments in each case. This standard tuning (table 7) provides an excellent control performance in the absence of multi-rate sampling and measurement delay in the outputs.

a) Servo problem with multi-rate sampling

Table 7: Standard tuning.

Parameters	
Prediction horizon (P)	10
Control horizon (M)	2
Move suppression factors	0.1 for all inputs
Penalties on the output deviations	20 for all outputs

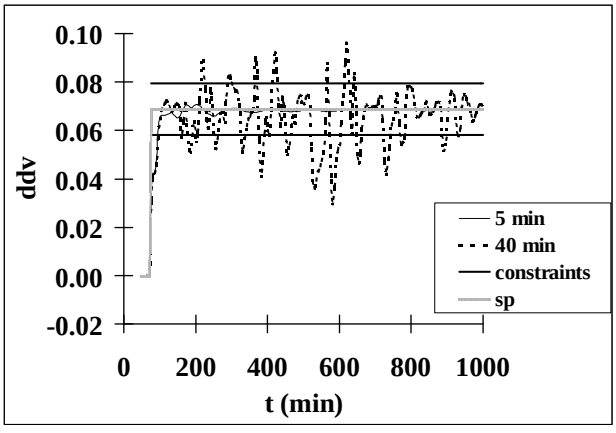

Figure 2: Temperature. Measurement intervals of 5 and 40 min for both M_w and X_{BT}. P=10, M=2 and control move weights equal to 0.1.

Figures 2-3 present simulation results with measurement intervals of 5 and 40 min for both molecular weight and comonomer content. In both cases, the standard tuning (table 7) was employed. Results show a sensible drop in the control performance with the occurrence of ringing (excessive oscillations) between sample points, owing to the increase in the measurement interval for the polymer properties (M_w and X_{BT}). On the other hand, Figure 4 shows that the performance improvement can be easily achieved through the increase in the prediction horizon and weights of control moves.

Some results presented show the occurrence of CV's values outside the specification limits (constraints). This fact is not related with the achievement of unfeasible solution for the optimization problem, since the hard constraints established according to Eq. (8) are imposed in the output predictions.

b) Servo problem with dead time

The same setpoint changes presented in table 4 were imposed considering a dead time equals to 30 min in the molecular weight and comonomer content measurements. Although the absence of multi-rate sampling, the Figure 5 presents the

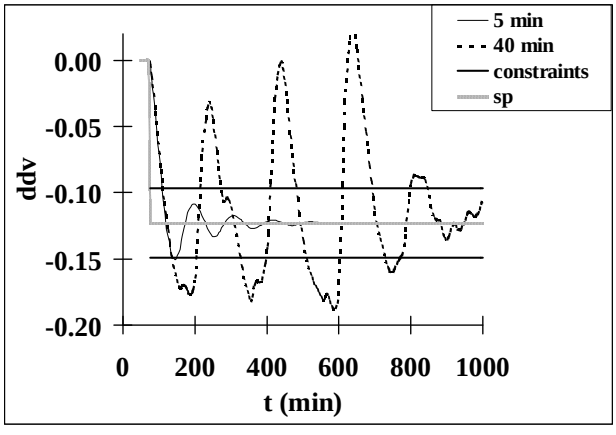

Figure 3: Molecular weight. Measurement intervals of 5 and 40 min for both M_w and X_{BT}. P=10, M=2 and control move weights equal to 0.1.

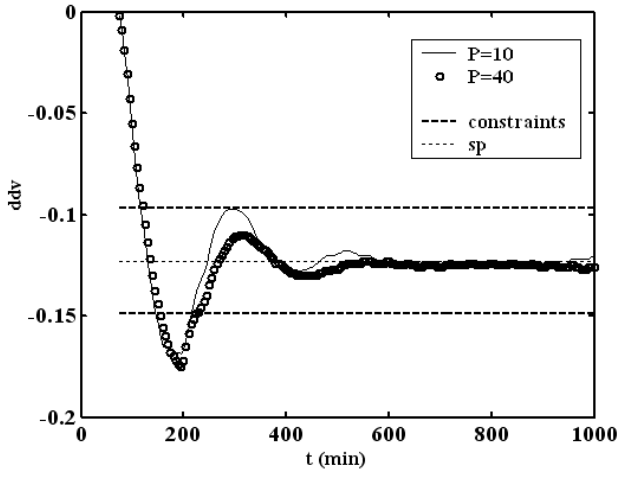

Figure 4: Molecular weight. Measurement intervals of 40 min for both M_w and X_{BT}. M=2 and control move weights equal to 0.5.

strong effect of dead time ("dt") on the control performance, with the occurrence of unstable behavior.

Despite the bad results achieved with the standard tuning, a sensible improvement can be obtained with a prediction horizon equals to 70 and weights of 0.5 or 1 for the control moves (Figure 6).

2.6.2 Regulatory problem

Temperatures of ethylene and solvent feed streams were considered as potential disturbances. No one setpoint change in the controlled variables was applied in this case.

Figures 7 and 8 present the temperature and comonomer con-

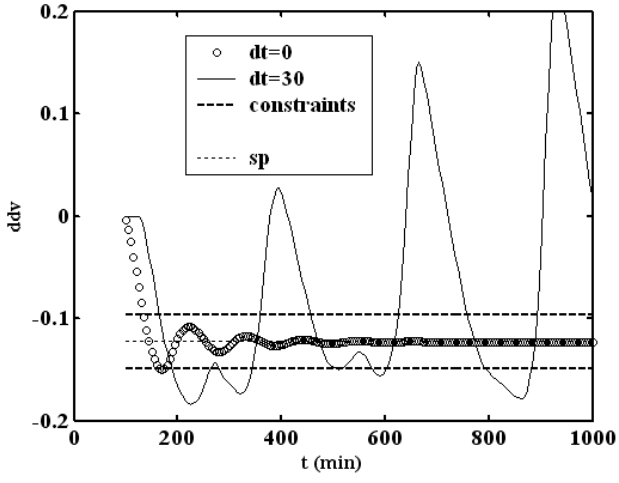

Figure 5: Molecular weight. Servo problem results without and with dead time of 30 min in the M_w and X_{BT}. P=10, M=2 and control move weights equal to 0.1.

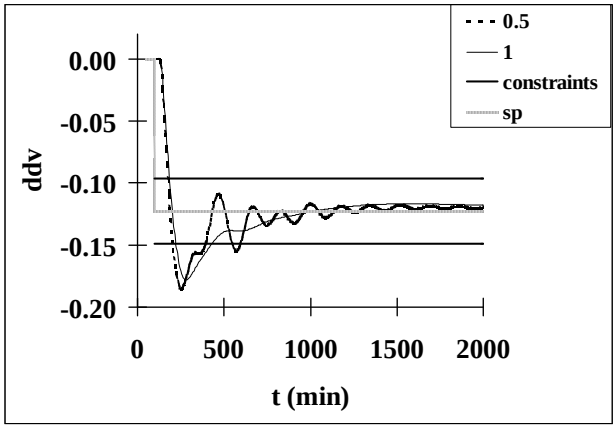

Figure 6: Molecular weight. Servo problem results with dead time of 30 min in the M_w and X_{BT}. P=70, M=2 and control move weights equal to 0.5 and 1.

tent profiles considering a dead time of 30 min in the polymer properties measurements, and the using of standard tuning (table 7). This test comprised the input of step perturbations of 20 % and 30 % on the ethylene and solvent temperatures, respectively. One more time, it can be detected a bad control performance with closed loop instability.

Figure 9 shows that the increase in prediction horizon and in the move suppression factors provides better results with the effective disturbance rejection. For the same step perturbations, simulation tests with multi-rate sampling in the controlled variables, without dead time, provided excellent results, even with the standard tuning (table 7).

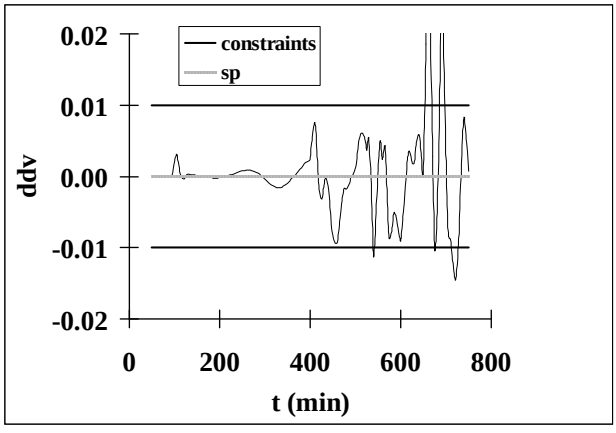

Figure 7: Temperature. Regulatory problem results with dead time of 30 min in the M_w and X_{BT}. P=10, M=2 and control move weights equal to 0.1.

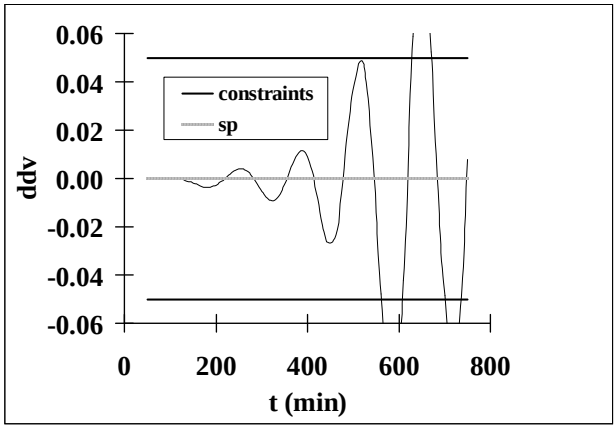

Figure 8: Comonomer content. Regulatory problem results with dead time of 30 min in the M_w and X_{BT}. P=10, M=2 and control move weights equal to 0.1.

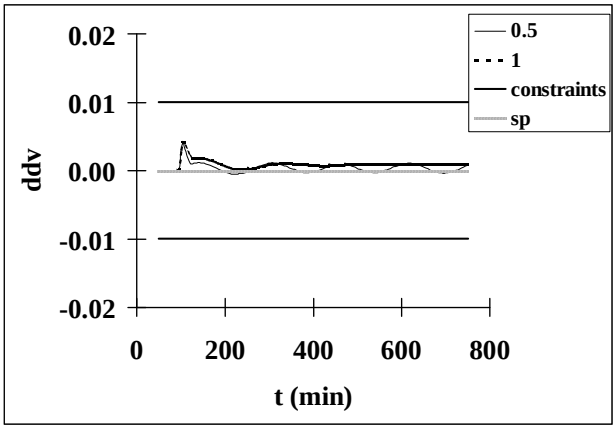

Figure 9: Temperature. Regulatory problem results with dead time of 30 min in the M_w and X_{BT}. P=70, M=2 and control move weights equal to 0.5 and 1.

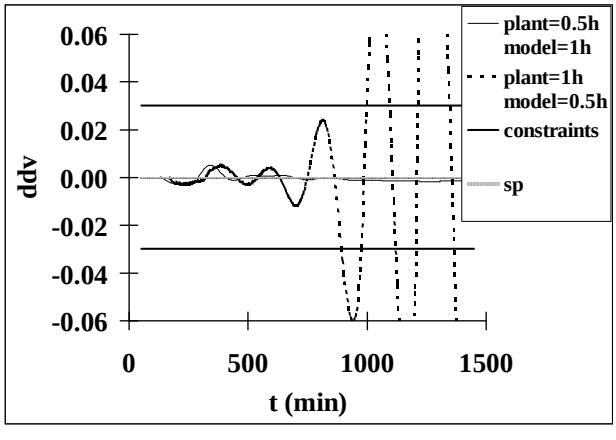

Figure 10: Molecular weight. Regulatory problem results with dead time error in the internal model. P=70, M=2 and control move weights equal to 0.5.

2.6.3 Uncertainty of dead time

Since the measurement delay in a real process is not exactly known and can vary over a very wide range, an uncertainty of this must be accounted in designing an NMPC controller.

Applying weights of 0.5 for the each control moves and the same horizons, Figures 10-11 present results with differences between the internal model dead time and the dead time effectively practiced in the process. A regulatory problem was considered with the input of a pulse perturbation on the solvent feed temperature. The results show that it is possible to achieve good performance even with a model dead time equals to 1 hour and a measurement delay in the process equals to 30 min. This also attests the robustness of the predictive control algorithm and denotes that the control performance, just as in the preceding sections, is directly related to increase of dead time practiced in the polymer properties measurements.

3 CONCLUSIONS

NMPC algorithm is applied to a slurry polymerization reactor where temperature, weight-average molecular weight and average fraction of comonomer incorporated into the polymer are the controlled variables. Considering the absence of multi-rate sampling in these outputs and delay in the polymer properties measurements, the simulation results for servo and regulatory problems show an excellent performance of the control algorithm, adopting a speed tuning with prediction and control horizons equal to 10 and 2, respectively, and move suppression factors two hundred times smaller than the

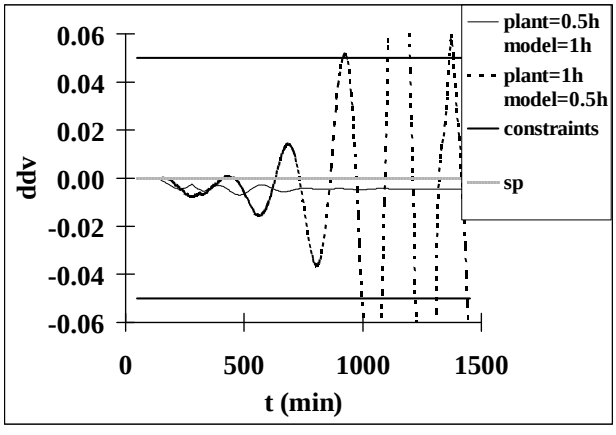

Figure 11: Comonomer content. Regulatory problem results with dead time error in the internal model. P=70, M=2 and control move weights equal to 0.5.

weights established for the output deviations.

The proposed control scheme represents advancement with regard to the actual scheme, enabling the effective control of macromolecular properties at desired values. Despite the other procedures previously published, based in a linear internal model, the use of NMPC enables the implementation of a more efficient controller, able to drive servo problems featured by large grade transitions. In this sense, this work also presents a proved strategy to handle the output restrictions during the transition.

The presence of considerable dead time or multi-rate sampling in the output measurements increases the complexity of the control problem. In this sense, the tuning procedure proposed in this work, comprising only the control move penalties and horizons adjustments, was capable to control all the outputs and enough to warrant the closed loop stability.

Still without dead time and multi-rate sampling, the excellent performance of NMPC together with the process stabilization through the use of long prediction horizons show that the internal neural model, trained for one step ahead prediction only, is perfectly suitable for the predictive control applications.

The presence of considerable delay in the polymer properties measurements produces a more complex control problem than with the existence of only multi-rate sampling. Although the adjustments of control move weights and/or prediction horizon were efficient in this case, the uncertainty and variability of dead time establishes the need of on-line estimators for the molecular weight and comonomer content that provide values of these outputs in the slurry stream. The success of a NMPC algorithm, applied to a slurry reactor and with direct control of mean molecular properties, depends strongly in how these variables must be measured or estimated.

Without the inclusion of dead time effect, the simulation results show that a control horizon equals to 2, a prediction horizon between 10 and 20 and control move weights equal to 0.5 can achieve satisfactory performance of NMPC for the system analyzed.

Another stage of polymerization engineering of this system could be reached through a direct control of end-use properties such as stiffness, impact strength and glass transition temperature, or definition of optimal operation conditions to achieve the desired values for these (reverse polymerization). In both cases, more complex relations, multivariable, must be determined between end-use and molecular properties such as molecular weight distribution (Latado et al., 2001, Valappil J. and Georgakis C., 2002, Farkas et al., 2004, Grosso and Chiovetta, 2005 and Asteasuain et al., 2003).

ACKNOWLEDGMENTS

The authors acknowledge the financial support provided by CNPq through a grant to C. Fontes as well as the technical support from Braskem Petrochemical Company.

NOMENCLATURE

Cd deactivated site.

$D\,(n,m)$ dead polymer chains with n monomer units and m comonomer units, mol/l;

d disturbance term used in conventional MPC feedback;

e deviations from the reference trajectory;

F_i feed flow rate of component i, ton/h;

k time in discrete system;

$K_{p_{ee}}, K_{p_{bb}}$ propagation rate constants, $l/\,(mol \cdot \min)$;

$K_{p_{eb}}, K_{p_{be}}$ propagation rate constants, $l/\,(mol \cdot \min)$;

K_{ts} rate constant for β-hydride elimination, $\min^{-1}$;

K_{th} rate constant for transfer to hydrogen, $l/\,(mol \cdot \min)$;

K_{tme} rate constants for transfer to monomer, $l/\,(mol \cdot \min)$;

K_{tmb} rate constants for transfer to monomer, $l/\,(mol \cdot \min)$;

K_{tcc} rate constant for transfer to cocatalyst, $l/\,(mol \cdot \min)$;

K_d deactivation rate constant, $\min^{-1}$;

M_w weight-average molecular weight;

M control horizon;

n_y number of output values in the neural network input layer;

nu_y number of past values of input u in the MISO model for output y;

P prediction horizon;

$P_1\,(n,m)$ living polymer chains with n monomer units and m comonomer units, with terminal monomer;

$P_2\,(n,m)$ living polymer chains with n monomer units and m comonomer units, with terminal comonomer;

$P\,(0,0)$ active site;

t_d dead time;

T_r reactor temperature, ^{o}C;

t time;

u manipulated variable;

X_{BT} average fraction of comonomer incorporated into the polymer;

y real process output (controlled variable);

$\hat{y}$ model output;

y_{ref} reference trajectory in MPC objective;

y_{sp} setpoint of output y;

Δu control move;

θ_u dead time of output related to input u;

α trajectory time constant;

Subscripts:

ET ethylene;

BT 1-butene;

C catalyst;

CC cocatalyst;

NX solvent (n-hexane);

H_2 hydrogen;

WC water to the reactor jacket;

WT water to the external heat exchangers;

i lower bound;

s upper bound.

j site type

ss steady state;

Superscripts:

j site type;

ad dimensionless variable.

Abbreviations

sp setpoint.

dt dead time.

MISO Multiple Input Single Output.

ddv dimensionless deviation variable.

CV controlled variable.

MV manipulated variable.

REFERENCES

Asteasuain, M., Pérez, M. V., Sarmoria, C. and Brandolin, A., "Modeling Molecular Weight Distribution, Vinyl Content and Branching in the Reactive Extrusion of High Density Polyethylene", *Latin American Applied Research*, 33, 241-249, (2003).

Diehl, M, Bock, H. G., Shloder. J. P., Findeisen, R., Nagy, Z., Allgower, F., "Real-time Optimization and Nonlinear Model Predictive Control of Processes Governed by Differential-Algebraic Equations", J. Process Control, 12, 577-585 (2002).

Doherty S. K., Gomm J. B. and Williams D., "Experiment Design Considerations for Non-Linear System Identification Using Neural Networks", *Computers Chem. Engng*, vol. 21, n^o 3, 327-346, (1997).

Dokucu, M. T., Park, Myung-June and Doyle F. J., "Multi-Rate model predictive control of particle size distribution on a semibatch emulsion copolymerization reactor", *Journal of Process Control*, 18, 105-120, (2008).

Dokucu, M. T., Park, Myung-June and Doyle F. J., "Reduced-order methodologies for feedback control of particle size distribution in semi-batch emulsion copolymerization", *Chemical Engineering Science*, 63, 1230-1245, (2008).

Embiruçu, M. and Fontes, C., "Multirate multivariable generalized predictive control and its application to a slurry reactor for ethylene polymerization", *Chemical Engineering Science*, 61, 5754-5767, (2006).

Farkas, E., Meszena Z. G. and Johnson, A., "Molecular Weight Distribution Design with Living Polymerization Reactions", *Industrial & Engineering Chemistry Research*, 43, 7356-7360, (2004).

Floyd S., K. Y.Choi , T. W. Taylor and W. H. Ray, "Polymerization of Olefins Through Heterogeneous Catalysis. III. Polymer Particle Modelling with an Analysis of Intraparticle Heat and Mass Transfer Effects", *J. Appl. Polym. Sci*., 32, 2935-2960, (1986).

Fontes, C. and Embiruçu, M., "Multivariable Correlation Analysis and Its Application to an Industrial Polymerization Reactor", *Computers & Chemical Engineering*, 25, 191-201, 2001.

Fontes C. and Mendes M., "Modeling and Simulation of an Industrial Slurry Reactor for Ethylene Polymerization", *Latin American Applied Research*, 31, 345-352, (2001).

Fontes, C. H. and Mendes, M. J., "Analysis of an Industrial Continuous Slurry Reactor for Ethylene-Butene Copolymerization", *Polymer*, 46, 2922-2932, (2005).

Fontes, C. H. O., Wakabayashi, C. and Embiruçu, M., "Analysis and Fuzzy Control of a Polymerization Reactor for Production of Nylon 6", In: XXII Interamerican Congress of Chemical Engineering, Buenos Aires, v. 1, 30-31, (2006).

Ghandi, R. and Mhaskar, P., "Safe-parking of nonlinear process systems", *Computers and Chemical Engineering*, 32, 2113-2122, (2008).

Gill P. E., Murray W. and Wright M. H., "Practical Optimization", Academic Press, Inc., (1981).

Grosso, W. E. and Chiovetta, M. G., "Modeling a Fluidized-Bed Reactor for the Catalytic Polymerization of Ethylene: Particle Size Distribution Effects". *Latin American Applied Research*, 35, 67-76, (2005).

Henson M. A., "Nonlinear Model Predictive Control: Current Status and Future Directions", *Comput. Chem. Engng.*, vol. 23, 187-202, (1998).

Hutchinson R. A., C. M. Chen and W. H. Ray, "Polymerization of Olefins Through Heterogeneous Catalysis. X. Modeling of Particle Growth and Morphology", *J. Appl. Polym. Sci.*, 44, 1389-1414, (1992).

Ibrehem, A. S., Hussain, M. A. and Ghasem, N. M., "Mathematical Model and Advanced Control for Gas-Phase Olefin Polymerization in Fluidized-bed Catalytic Reactors", *Chinese Journal of Chemical Engineering*, 16 (1), 84-89, (2008).

Jeong, B. G., Yoo K. Y. and Rhee H. K., "Nonlinear Model of a Continuous Methyl Methacrylate Polymerization reactor", *Industrial & Engineering Chemistry Research*,40, 5968-5977, (2001).

Kiparissides C., "Polymerization Reactor Modeling: A Review of Recent Developments and Future Directions", *Chem. Eng. Sci.*, 51(10), 1637-1659, (1996).

Latado, A., Embiruçu, M., Mattos, A. G., Pinto, J. C., "'Modeling of end-use Properties of Poly(propylene/ethyelene) Resins", *Polymer Testing*, 20, 419-439, (2001).

Meadows E. S. and Rawlings J. B., in Henson M. e Seborg D., "Nonlinear Process Control", Prentice-Hall, Inc., (1997).

Nagy, Z. K., Mahn, B., Franke, R. and Allgower, F., "Evaluation study of an efficient output feedback nonlinear model predictive control for temperature tracking in an industrial batch reactor", 15, 839-850, (2007).

Ozkan G., Ozen S., Erdogan S., Hapoglu H and Alpbaz M, "Nonlinear Control of Polymerization Reactor", *Comput. Chem. Engng.*,vol. 25, 757-763, (2001).

Penlidis, A., Ponnuswamy, S. R., Kiparissides, C., and O'Driscoll, K. F., "Polymer Reaction Engineering: Modelling Considerations for Control Studies", *The Chemical Engineering Journal*, 50, 95-107, (1992).

Qin S. J. and Badwell T. A., "An Overview of Industrial Model Predictive Control Technology", *Aiche Symp. Ser*., 93, 232-256, (1997).

Qin S.J. and Badgwell, T.A., "An Overview of Nonlinear Industrial Model Predictive Control Applications". In: Nonlinear Model Predictive Control. Allgöwer, F., A. Zheng (Eds.). *Progress in Systems and Control Theory Series*, v. 26, Switzerland: Birkhauser Boston, (2000).

Ray W. H., "Modelling of Addition Polymerization Processes", *Can. J. Chem. Eng.*, 69, 626-629 (1991).

Rovaglio, M., Algeri, C and Manca D., "Dynamyc Modeling of a Poly (ethyelene terephtalate) Solid-State Polymerization Reactor II: Model Predictive Control", *Industrial & Engineering Chemistry Research*, 40, 4267-4277, (2004).

Schnelle P D. and Rollins D., “Industrial Model Predictive Control Technology as Applied to Continuous Polymerization Processes”, *ISA Transactions*, vol. 36, no 4, 281-292, (1998).

Soares J. B. P. and A. E. Hamielec, “General Dynamic Mathematical Modelling of Heterogeneous Zielger-Natta and Metallocene Catalyzed Copolymerization with Multiple Site Types and Mass and Heat Transfer Resistances”, *Polymer Reaction Engineering*, 3(3), 261-324, (1995).

Soares J. B. P. and A. E. Hamielec, “”Copolymerization of Olefins in a Series of Continuous Stirred-tank Slurry-Reactors using Heterogeneous Ziegler-Natta and Metallocene Catalysts. I. General Dynamic Mathematical Model”, *Polymer Reaction Engineering*, 4(2&3), 153-191, (1996).

Su H. T. and McAvoy T. J., in Henson M. e Seborg D., “Nonlinear Process Control”, Prentice-Hall, Inc., (1997).

Valappil, J., Georgakis, C., “Nonlinear Model Predictive Control of end-use Properties in Batch Reactors”, *AIChE Journal*, 48, no 9, 2002.